



---

**SYNTHESIS, CHARACTERIZATION AND WATER ABSORPTION CAPACITY OF CHITOSAN-TiO<sub>2</sub> NANOCOMPOSITE AS AN EFFECTIVE WATER SORBENT**

\*<sup>1,2</sup>P.A. Francis, <sup>1</sup>F.G. Okibe, <sup>1</sup>E.B. Agbaji and <sup>3</sup>F. N. Bernice

<sup>1</sup>Department of Chemistry, School of Physical Sciences, Ahmadu Bello University, Zaria, Nigeria

<sup>2</sup>National Examinations Council, Minna, Nigeria.

<sup>3</sup>Department of Wood Science, Faculty of Forestry, Federal University of Agriculture, Makurdi, Nigeria

\*Corresponding Author: yamashmily2@gmail.com

**ABSTRACT**

In the present study, chitosan from mushroom were prepared and used to synthesize chitosan-TiO<sub>2</sub> by mixing TiO<sub>2</sub> and chitosan in 1:1 and 1:4 ratios via green sol-gel nanocomposites synthesis method. The characterization of the prepared nanocomposites was carried out by advanced analytical tools such as Fourier Transform Infra-Red spectroscopy (FT-IR), X-ray diffraction (XRD), Transmission Electron Microscope (TEM) and Scanning Electron Microscope (SEM). The water absorption capacity (WAC) test of the nanocomposites was carried out to determine their suitability as moisture/water sorbent materials in stored grains and animal feed additives. The results of water absorption studies carried out showed that, CTNC (1:4) absorbed 34% of water after 16hrs of exposure while CTNC (1:1) had 31% optimum value. The WAC of the nanocomposites was found to be a function of time and amount of nanocomposites investigated.

**Key words:** Chitosan, Mushroom, FT-IR, SEM, TEM, Water absorption capacity

**INTRODUCTION**

In many parts of Africa, the major food crops such as cereal grains are normally seasonal crops. Consequently the food produced in one harvest period, which may last for only a few weeks, must be stored for gradual consumption until the next harvest, and seed must be held for the next season's crop. Therefore the principal aim of any storage system must be to maintain the crop in prime conditions for as long as possible [1]. Any storage and handling methods adopted should minimize losses and retain the physical and nutritional qualities of these grains. But since under humid and warm conditions, harvested grains are susceptible to molding and rapid deterioration, mitigation strategies that include the inclusion of natural,

green and cheap materials that has the ability to eliminate moisture and inhibit the activities of microorganisms and therefore, preserving grains and feed at hermetic conditions could serve as a feasible and economical solution for feed and grain preservation and storage in warm and moist climes [2].

Chitosan, poly [ $\beta$ -(1-4)-2-amino-2-deoxy-D-glucopyranose], is one of the most important cationic pseudo-linear polysaccharides [3]. Chitosan is the second most abundant and available biopolymer in nature after cellulose. It is a nontoxic, biocompatible, and biodegradable biopolymer derived from polysaccharide chitin which is extracted from the structural components of fungi i.e mushroom, marine organisms such as, shrimps, lobsters, and crabs [4]. In its unit structure, it contains high reactive functional groups (hydroxyl group -OH, and amino -NH<sub>2</sub>) which are responsible for donating a lone pair of the electron, high solubility in a diluted acidic solvent, the formation of the coordination bonds and make the modification of chitosan easy [5].

In spite of the significant properties of chitosan, some drawbacks limit its performance and applicability. These limitations include solubility in acid, low mechanical strength and low surface area [6]. This necessitated the chemical modification of chitosan such as chemical cross-linking to increase its stability in acidic solutions, mechanical strength and surface area [7], or composition with nanomaterials to enhance physiochemical properties such as surface area, porosity and mechanical [7].

It has been reported that, crosslinked chitosan-TiO<sub>2</sub> (CTNC) nanocomposite has superior sorbent, anti-bacterial, anti-fungal, anti-coagulant properties [8-9].

In this study TiO<sub>2</sub>-chitosan nanocomposites was synthesized using different ratios of chitosan synthesized from mushroom and different techniques were employed to characterize the nanocomposite powders i.e FTIR, XRD, SEM, and TEM. The purpose of the current study was to examine the characteristics and water removal capacity of chitosan-TiO<sub>2</sub> nanocomposites that makes it suitable as grains and feeds storage additives.

## **MATERIALS AND METHODS**

### ***Preparation of Chitosan from commercial mushroom***

The protocols as described by Mohammed *et al* [10] were used to synthesis and characterize CTNCs from mushroom.

### **Demineralization**

The method described by Mohammed *et al.* [10] was used with slight modifications. Briefly, 50 g of dried and pulverized commercial mushroom was weighed and put into a 500 mL beaker glass, then 1M HCl solution with a ratio of 1:10 (w/v) was added. The mixture was stirred with a magnetic stirrer at room temperature for 3 hours and then filtered with Whatman 41  $\mu\text{m}$  filter paper while washing continuously with distilled water until no residual chloride ion remained in the samples. The washing process was stopped when the pH was neutral. The residue was dried in an oven (70°C) until constant weight.

### **Deprotonation**

After demineralization step, the dried residue from demineralization step was put into a 500 mL beaker and then 1 M NaOH solution at a ratio of 1:10 (w/v) was added. The mixture was heated and stirred at 60°C on a hotplate for 1 hour and then filtered with Whatman filter paper. The residue was washed with distilled water until neutral pH, and then dried in an oven at 70 °C until constant weight, the product here is chitin.

### **Deacetylation**

The deacetylation of chitin produces Chitosan. In this step, the chitin formed from the deprotonation step was put into glass beaker and then 1 M NaOH solution at a ratio of 1:10 (w/v) was added. The mixture was heated and stirred at 90 °C on hotplate for 2 hours. The mixture was filtered with Whatman 41  $\mu\text{m}$  filter paper and the residue was washed with distilled water until the residue namely chitosan became neutral. The formed Chitosan was dried in an oven at 70 °C until dry to constant weight.

### **Synthesis of Chitosan-TiO<sub>2</sub> nanocomposite**

For the Chitosan synthesis, the method described by Mohammed *et al.* and Li *et al.* [10-11] was adopted with slight modification. Briefly, nanocomposites were synthesized by incorporating various amounts of nano-sized TiO<sub>2</sub> particles into Chitosan solutions of different concentrations. 10 g of chitosan was added into 100 mL of 0.1 M HCl solution in 250 mL beaker glass, while continuously stirring until it dissolved evenly and then TiO<sub>2</sub> particle was added in a ratio of 1: 1 (w/w) and then stirred continuously for 12 hrs. The product was then filtered with Whatman filter paper to obtain the nanocomposite Chi-TiO<sub>2</sub> as residue on the filter paper. This process was repeated for the other ratios. The nanocomposite was washed with distilled water until the filtrate became neutral.

### Characterization of CTNC

Scanning electron microscopic observation of varied CTNC ratios were performed as described by Yu *et al.* [12] with a JEOL-JSM (Hitachi, Tokyo, Japan) JSM-7600F Scanning Electron Microscope.

Transmission Electron Microscope observation of varied Chi-TiO<sub>2</sub> nanocomposites was performed as described by Yu *et al.*[12] with Nanomil (Hitachi, Tokyo, Japan) Transmission Electron Microscope.

Fourier transform infrared spectra were determined and analysed as described by Yu *et al.* [12] with an FTIR spectrometer (Nicolet iS10), while pellets were scanned at 4 cm<sup>-1</sup> resolution with 100 scans in the spectral range of 4000-500 cm<sup>-1</sup> at room temperature.

X-ray diffraction analysis were performed according to the method described by Li *et al.*[11] by using RIGAKU diffractometer with a detector operating under a voltage of 40.0 kV and a current of 30.0 mA using Cu/K $\alpha$  radiation. The recorded range of 2 $\theta$  was 5–60°, and the scanning speed was 6°/min.

### Water Absorption Studies

Water uptake capacity of nanocomposites was done according to the method described by ASTM, D570-98 [13]. Briefly, samples with varied weights (1.0, 2.5, 5.0 g) were immersed into separate beakers containing 25ml of water kept in a thermostatic water bath set at room temperature (32°C) and high temperature (42°C). These samples were periodically removed from the water bath after a definite time intervals (1, 2, 4, 8, 16 hrs). Then weighed after blotting with filter paper.

The percentage weight gain at any time, 't', as a result of solution absorption was determined using the equation given below.

$$WAC\% = \left[ \frac{W_{wet} - W_{dry}}{W_{dry}} \right] \times 100$$

Where, W wet = Weight of the sample at different time intervals (after soaked in water).

Wdry = Initial weight of the dry sample respectively.

---

## RESULTS AND DISCUSSION

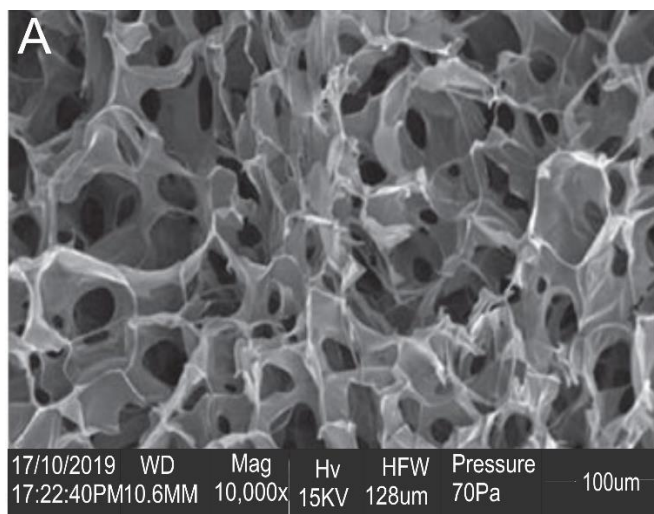


Figure 1: SEM photograph of CTNC (1:1)

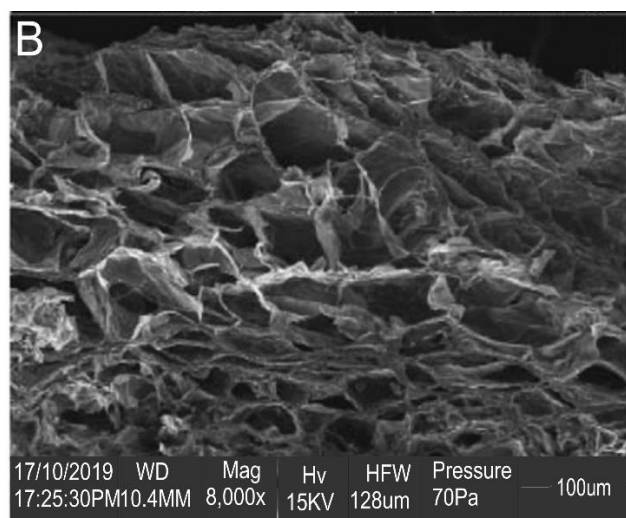
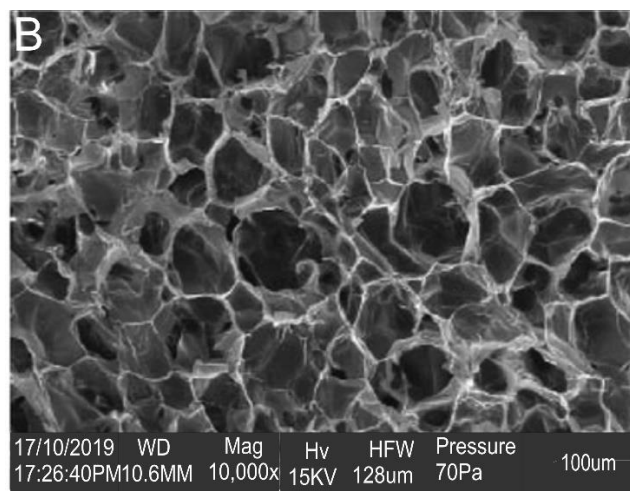


Figure 2: SEM photograph of CTNC (1:4)

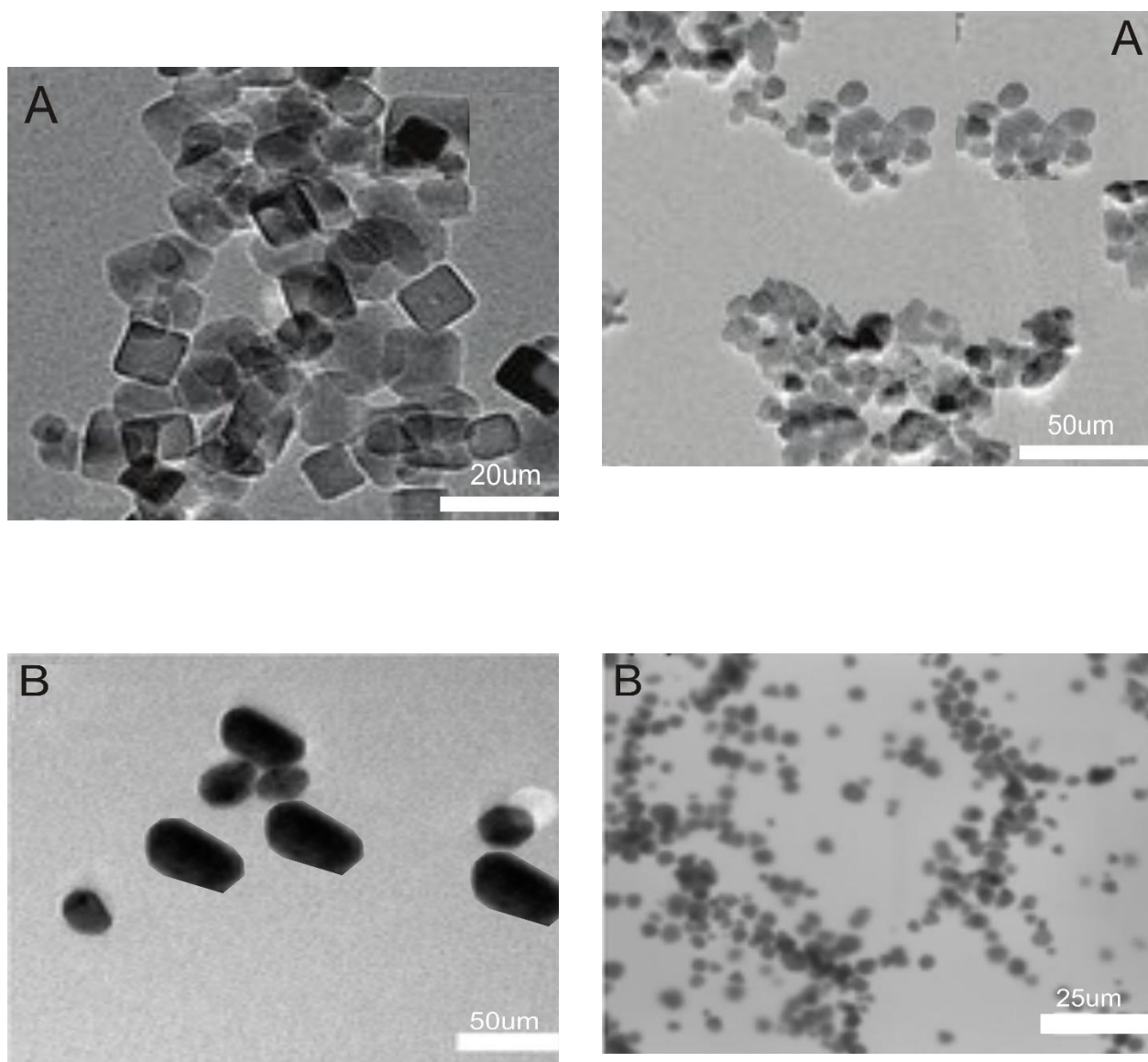


Figure 3: TEM micrograph of CTNC (1:1 and 1:4)

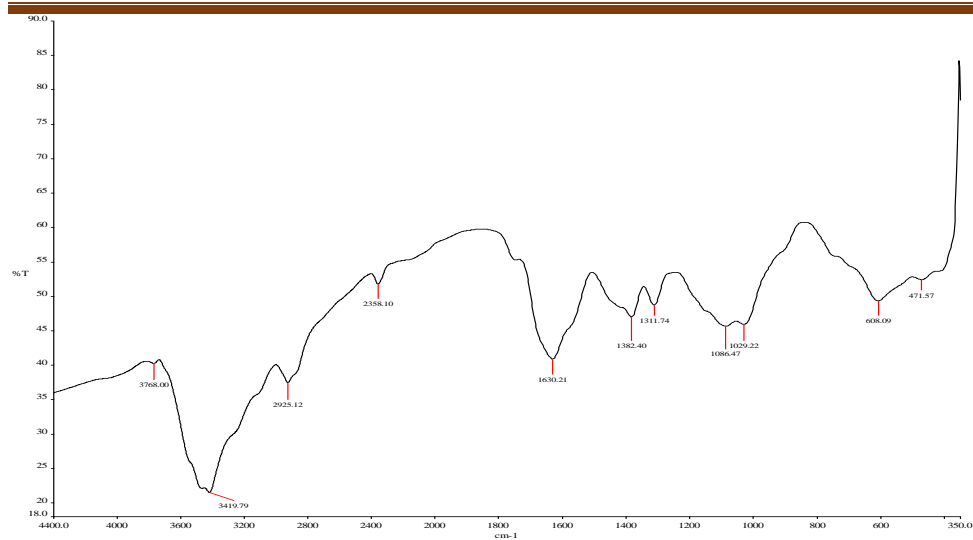


Figure 4: FT-IR Pattern of CTNC (1:1)

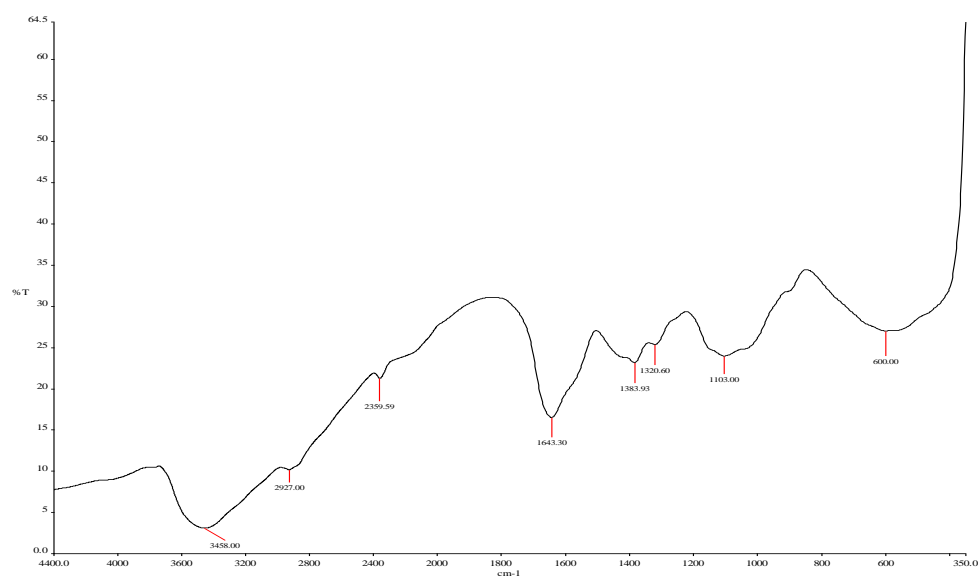


Figure 5: FT-IR Pattern of CTNC (1:4)

---

<b>Sample</b> : Sample A	<b>File</b> : Sg2~1.ASC	<b>Date</b> : Oct 18 7:34:30	<b>Operator</b> :
<b>Comment</b> : Qualitative	<b>Memo</b>		
<b>Method</b> : 2nd differential	<b>Typical width</b> : 0.065 deg.	<b>Min. Height</b>	<b>350:00 c p s</b>

---

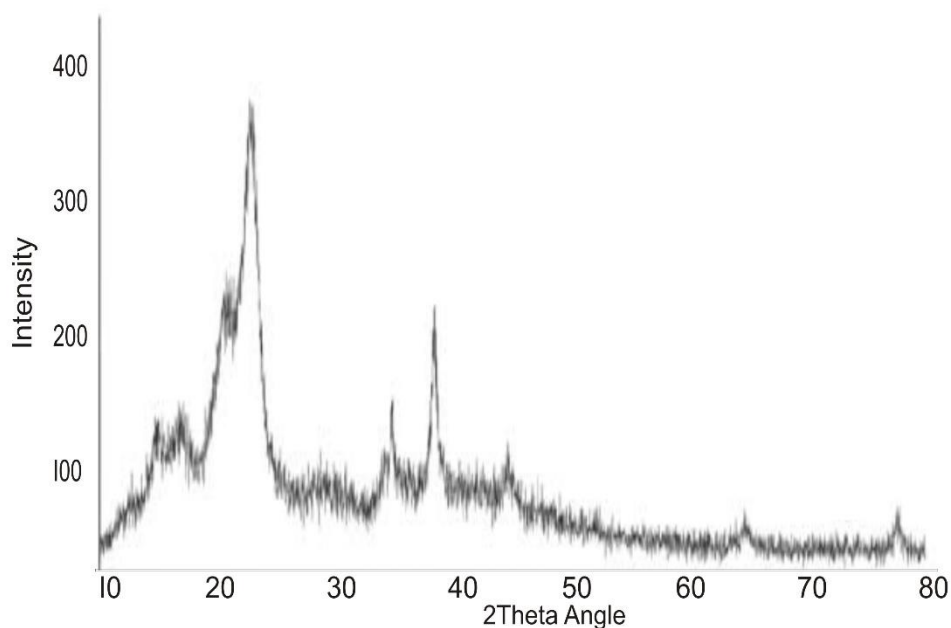


Figure 6: XRD Pattern of CTNC (1.1)

---

<b>Sample</b> : Sample B	<b>File</b> : Sg2~1.ASC	<b>Date</b> : Oct 17 7:44:20	<b>Operator</b> :
<b>Comment</b> : Qualitative	<b>Memo</b>		
<b>Method</b> : 2nd differential	<b>Typical width</b> : 0.065 deg.	<b>Min. Height</b>	<b>400:00 c p s</b>

---

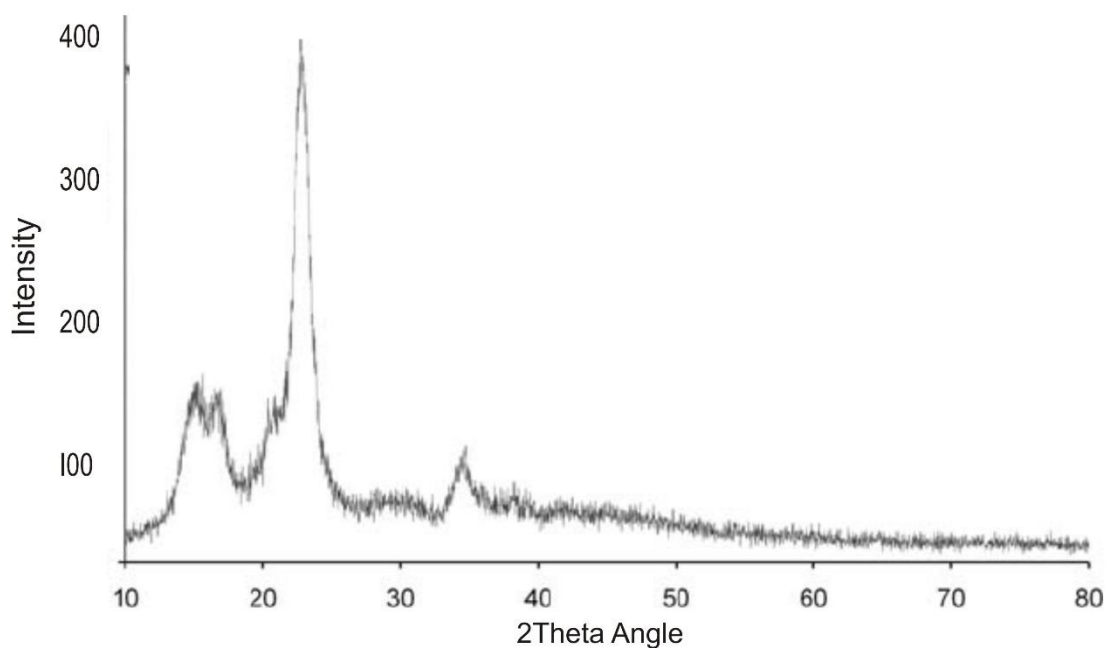


Figure 7: XRD Pattern of CTNC (1:4)

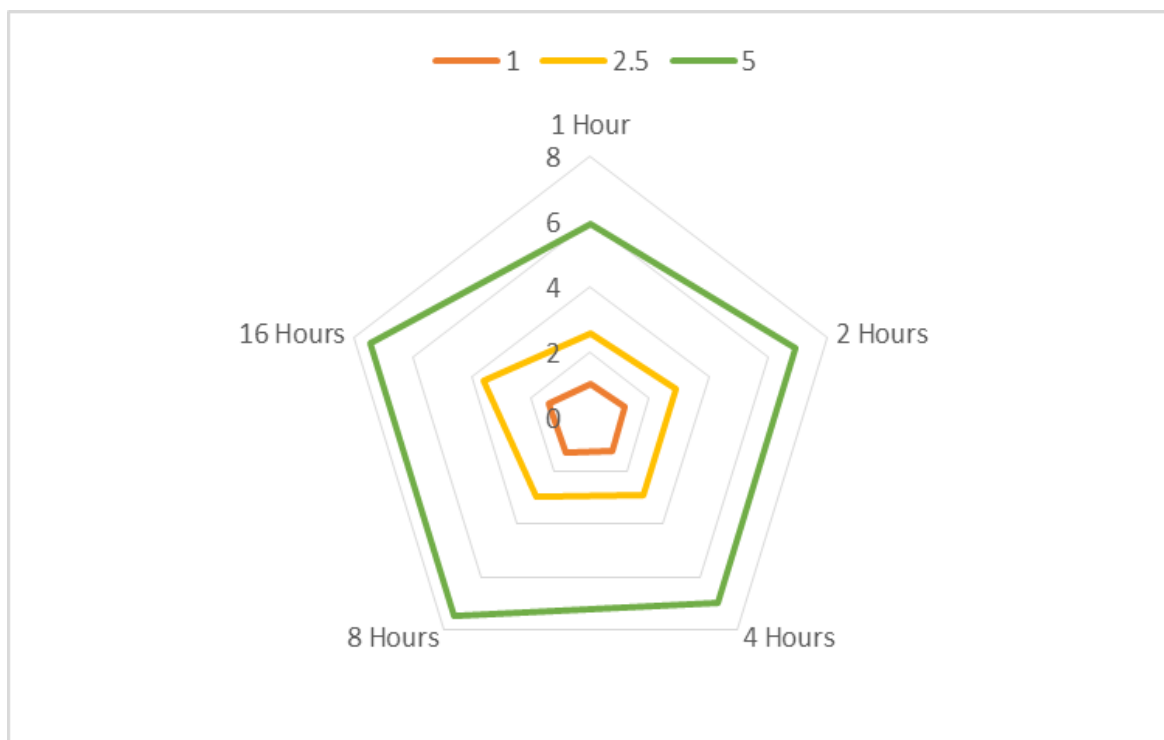


Figure 8: RADAR chart of water absorption capacity of CTNC (1:4)

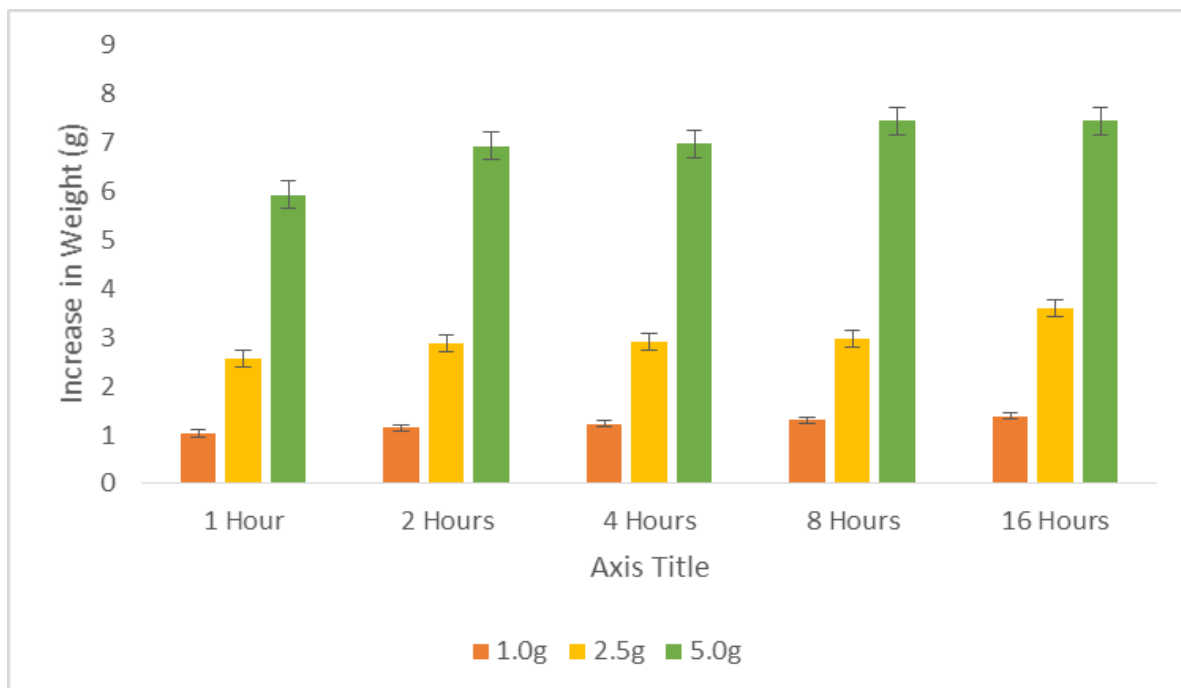


Figure 9: Bar chart for water absorption capacity of CTNC (1:4)

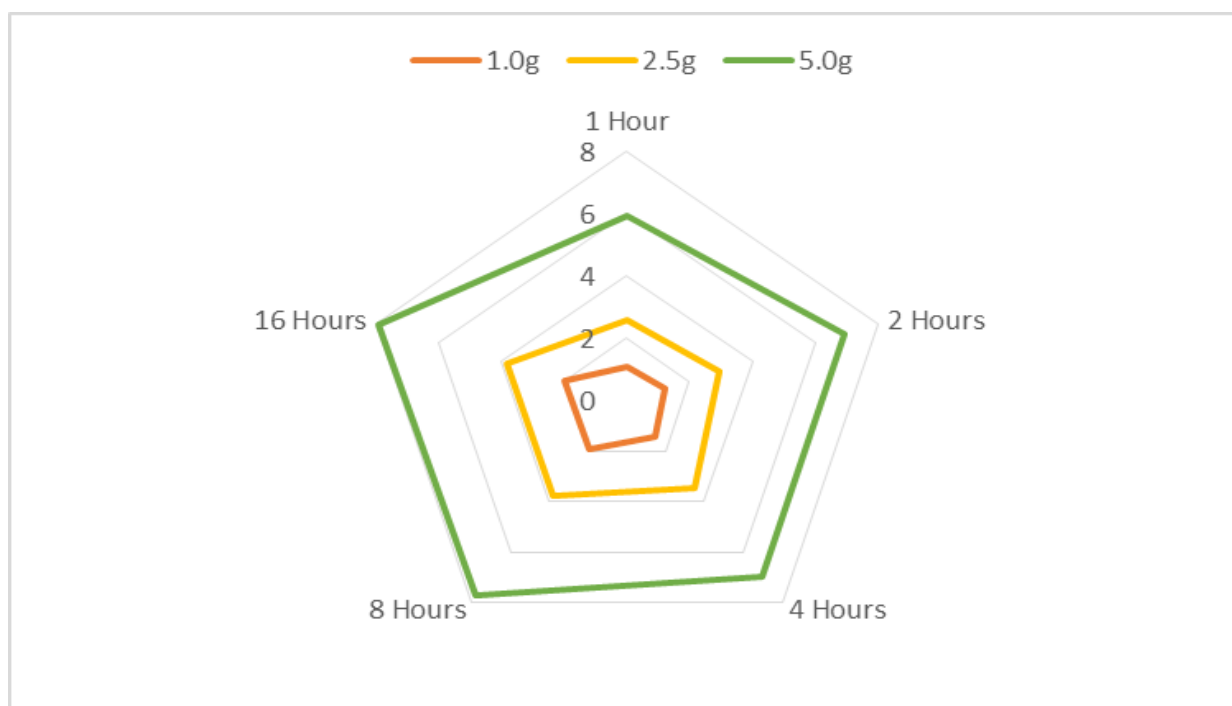


Figure 10: RADAR chart of water absorption capacity of CTNC (1:1)

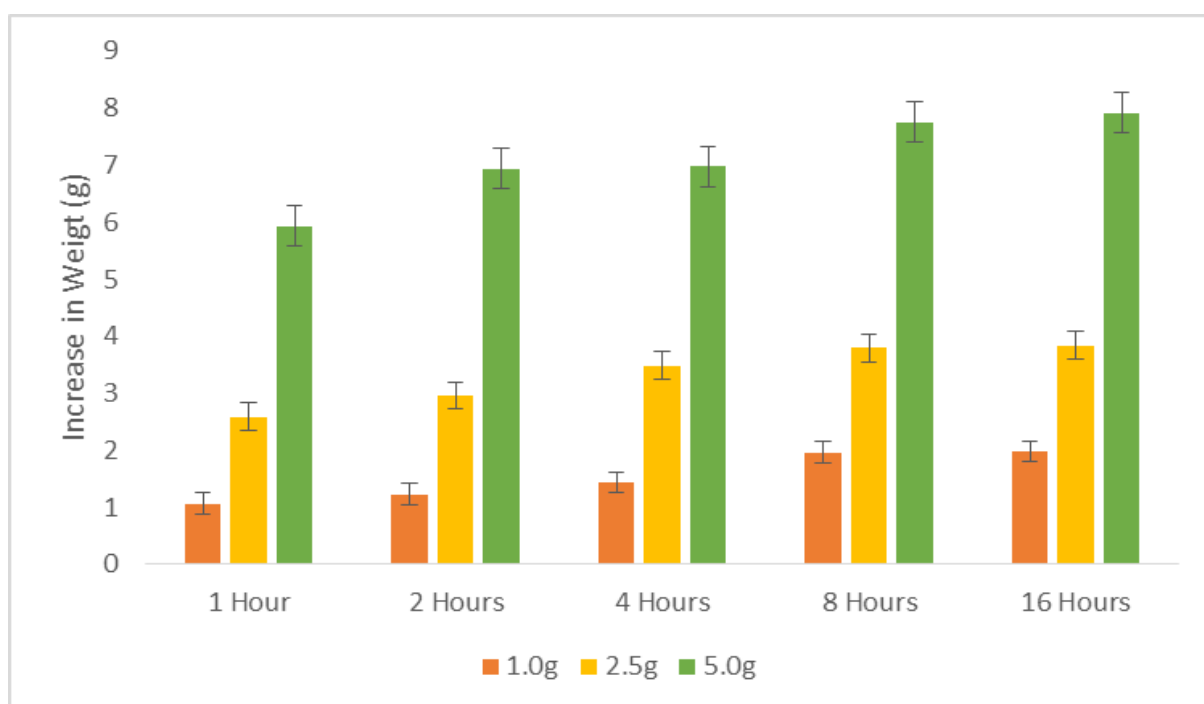


Figure 11: Bar chart for water absorption capacity of CTNC (1:1)

The SEM photographs of varied Chi-TiO<sub>2</sub> nanocomposites are shown in Figs. 1 and 2 respectively. The CTNCs were dense, flat but smooth with some vicious pores. Although the

image of the CTNC (1:4) is similar to that of the CTS on the same scale, CTNC (1:1) showed a better modified structure. The results suggested that the electrostatic repulsive forces between the polymer chains of CTS and the surface of the TiO<sub>2</sub> nanoparticles may play an important role in breaking down the undesirable agglomeration of inorganic nanoparticles.

The performance CTNCs in this study have been found to be correlated with their structural and morphological features such as its crystalline phase, crystallite size, surface area, pore structure, phase purity and visible light absorbing capacity reported in similar studies [14, 15]. The water absorption capacity of CTNC has been suggested to be due to both their size and high surface-to-volume ratio [16-17]. It is worthy of note that, CNC a natural reactive biopolymer and its hydrogel structure makes it possible to form various shapes, which could possibly improve efficiency of CTNC by modification of its surface.

Images obtained from SEM analysis indicate that, the TiO<sub>2</sub> nanoparticles uniformly dispersed in the CTS increased its surface area. Indeed, under the electrostatic repulsion forces between inorganic nanoparticles and the polymer matrix, the flexible chain of CTS molecules can be fully stretched out, and the dispersion of nanoparticles in the polymer matrix can be improved. This provides the hybrid film with a stable open network structure and a larger surface area, enabling it to carry large amounts of positive charges and bulk materials. Indeed, microsphere materials that provide more adsorption sites for adsorbate are favourable for storage and other technological application because of their high surface area, compared with nanoparticles that present some drawbacks because of their small sizes, which are commonly in the form of unstable aggregate in water. Therefore, it could be suggested that porous structure of CTNC makes it more efficient and suitable for water absorption and the adsorption of other organic pollutants [18].

### **Transmission Electron Microscopy images of CTNCs**

The images of the TEM analysis for the synthesized CTNCs (1:1 and 1:4) were presented in Figure 3. TEM analysis provides the interaction of electrons with the specimen, morphologic and compositional information of nanomaterials. Also, the particle sizes and shape of the CTNC samples were determined from the TEM images. The images presented agree with the results obtained from the XRD analysis. The images revealed that, the nanocomposites powders are octahedron with anatase TiO<sub>2</sub> in shape and their average size is about 12.1 nm. Generally, a homogenous dispersion and uniform particle features, with particle sizes of 5-30 nm for TiO<sub>2</sub> are shown. It has been demonstrated that almost 90% of the TiO<sub>2</sub> are 10-20 nm.

TEM results confirmed that, for the CTNCs prepared via sol-gel method from the Ti[OCH(CH<sub>3</sub>)<sub>2</sub>]<sub>4</sub> precursor TiO<sub>2</sub>, all samples have an anatase phase and this might be related to the sol-gel synthesis method being applied in the preparation of the nanocomposites. In this process, the nucleation of TiO<sub>2</sub> is controlled by increasing the temperature and pH of media, amount of precursor and therefore resulting in shorter induction time for the nucleation and faster growth rate [19]. An important factor that contributes to the highly efficient water absorption of the CTNC is the modifications on the surface or bulk ratio, thus modifying the significance of both volume and surface electron-hole recombination, as well as the optical and electronic properties of the nanocomposites. These results showed that, the diameter of CTNCs were influenced by the ratios of CTS and TiO<sub>2</sub> used. The agitation in the system or stirring time of the reaction also impacted the form and size of nanocomposites produced.

### **FTIR spectra of CTNCs**

The FT-IR spectra of CTNCs are shown in Fig. 4 and 5 respectively. The main peaks for CTS can be assigned as follows: 1597 cm<sup>-1</sup> (NH<sub>2</sub> deformation vibration), 1261 cm<sup>-1</sup> (O-H bending vibration), 3419 cm<sup>-1</sup> (N-H and O-H stretching vibration), 1029 cm<sup>-1</sup> and 1028 cm<sup>-1</sup> (C-O stretching vibration of C3 secondary and C6 first hydroxyl), while 1103 cm<sup>-1</sup> and 896 cm<sup>-1</sup> are characteristic bands of glucosidic bond in CTS. The peaks of TiO<sub>2</sub> at 1093, 2851, and 3429 cm<sup>-1</sup> were ascribed to surface hydroxyl groups and adsorbed water molecules and the band at 471-608 cm<sup>-1</sup> correspond to the Ti=O=Ti stretching vibration mode.

Comparison of the FTIR spectra revealed CTNC had most of the characteristic adsorption peaks of CTS and TiO<sub>2</sub> but displayed some slight changes in the intensity of the peaks assigned to the amino and hydroxyl groups of CTS and the surface hydroxyl groups of TiO<sub>2</sub>. Furthermore, compared to CTS and TiO<sub>2</sub>, some peaks such as the C-O stretching vibration of C3 in 1029 cm<sup>-1</sup> has some red shift, while several peaks such as 2925 cm<sup>-1</sup>, 1630 cm<sup>-1</sup>, 1103 cm<sup>-1</sup> and 896 cm<sup>-1</sup> disappeared, demonstrating that -NH<sub>2</sub> and glucosidic bond are not involved in the activities of CTNC. These structural changes revealed the formation of hydrogen bonds between -NH<sub>2</sub> groups of CTS and -OH groups on the surface of the TiO<sub>2</sub> nanoparticles, which may attribute to its improved water absorption capacity.

### **XRD Analysis of CTNCs**

The results for the XRD analysis of synthesized CTNCs were shown in Figs 6 and 7. They indicated that, the XRD pattern of chitosan is usually represented by the distinct crystalline

peaks  $2\theta = 9.71^\circ$  and  $20.38^\circ$ , which are assigned to (020) and (100) reflections. This is because plenty of hydroxyl and amino groups of the CTS structure could form stronger intermolecular and intramolecular hydrogen bonds, while certain regular structure resulting in CTS molecules could form crystalline regions very easily. However, the introduction of TiO<sub>2</sub> particles into the CTS phase resulted in the disappearance of both CTS peaks. In this study, the synthesized CTNC exhibited the typical characterization peaks of TiO<sub>2</sub>, with a new peak around  $40.3^\circ$ . Therefore, it could be hypothesized that TiO<sub>2</sub> particles in both 1:1 and 1:4 nanocomposite, interfered with the ordered packing of polymer chains by hydrogen bonding due to the substitution of hydroxyl and amino groups, which led to the decrease in the CTS crystallinity but not the crystalline structure of TiO<sub>2</sub> [19].

### **Water Absorption Capacity of the Nanocomposite**

The results of water absorption values of the synthesized CTNCs (1:1 and 1:4 w/w) are presented in figures 8 to 11 respectively. From the results, 1.0 g of CTNC (1:1) had WAC of 3%, 4%, 10% after immersion in water for 1, 2, 4, 8, and 16 hrs respectively; 2.5 g had WAC of 28%, 28.5%, 31%, 34%, for 1, 2, 4, 8, and 16 hrs while 5.0 g had 18%, 28%, 30%, 31% for 1, 2, 4, 8, and 16 hrs respectively. CTNC 1:4 had similar WAC pattern but the 2.5 g and 5.0 g performed better than those of CTNC (1:1). From the result, it was observed that the WAC of CTNCs increases significantly as the amount and the period (time) of immersion increases, but, WAC decreases proportionally as the amount of TiO<sub>2</sub> increases. This may be due to the fact that, the addition of TiO<sub>2</sub> decreased the average size of the polymer particle and then decreased the free volume and voids by increasing the affinity of CTNC [17-20].

### **CONCLUSION**

This study reports the synthesis and characterization of the CTNCs, which had better WAC when time of exposure and amount of sorbent increased. These economical, environmentally friendly and sustainable agricultural sorbent materials were found useful for the control of moisture content in stored grains. Furthermore, the results indicated that the improved WAC of nanocomposites in particular at the ratio of 1:4 may be attributed to the synergistic interaction between Chitosan and TiO<sub>2</sub>, which resulted in the change in the surface morphology, physicochemical properties, structure and functions.

## REFERENCES

1. FAO/WHO, (2017). Evaluation of Certain Contaminants in Food and Food Additives. WHO technical report series, Rome, Italy.
2. McKeivith, B. (2004). Nutritional aspects of cereals. *Nutrition Bulletin*, 29(2), 111-142.
3. Saifuddin, N., Nian C., Zhan L. & Ning K. (2011) Chitosan-silver nanoparticles composite as point-of-use drinking water filtration system for household to remove pesticides in water. *Asian Journal of Biochemistry*; 6:142–59.
4. Younes, I. & Rinaudo M. (2015). Chitin and chitosan preparation from marine sources. Structure, properties and applications. *Marine Drugs*. 13:1133–74.
5. Miretzky, P. & Cirelli A.F. (2009). Mercury (II) removal from water by chitosan and chitosan derivatives: a review. *Journal of Hazardous Materials*; 167:10–23.
6. Vakili, M., Rafatullah, M., Salamatinia, B., Abdullah, A. Z., Ibrahim, M. H. & Tan, K. B. (2014) Application of chitosan and its derivatives as adsorbents for dye removal from water and wastewater: A review. *Carbohydrate Polymer*; 113:115–30.
7. Li X-Q. & Tang R-C. (2016). Crosslinked and dyed chitosan fiber presenting enhanced acid resistance and bioactivities. *Polymers*; 8:119.
8. Nishad, P. A. Bhaskarapillai, A. & Velmurugan, S. (2014). Nano-titania-crosslinked chitosan composite as a superior sorbent for antimony (III) and (V). *Carbohydrate Polymer*; 108:169–75.
9. Bagheri, S., Hir, Z. A. M., Yousefi, A. T., & Hamid, S. B. A. (2015). Progress on mesoporous titanium dioxide: synthesis, modification and applications. *Microporous and Mesoporous Materials*, 218, 206-222.
10. Mohammed, N.I.A, Nurhidaytullaili, M. J., Samira, B. & Amin, T. Y. (2015). Applications of Chitosan-TiO<sub>2</sub> nanocomposite as adsorption and photocatalytic precursors. *Inorganic Reviews*. DOI 29-i515/reviews 2015-0005.
11. Li, B., Liu, B. P., Shan, C. L., Ibrahim, M., Lou, Y. H., & Wang, Y. L. (2013). Antibacterial activity of two chitosan solutions and their effect on rice bacterial leaf blight and leaf streak. *Pest Management Science*, 69, 312-320.
12. Yu, B. Y., Leung, K. M., Guo, Q. Q., Lau, W. M., & Yang J. (2011). Synthesis of Ag-TiO<sub>2</sub> composite nano thin film for antimicrobial application. *Nanotechnology*, 22, 115603.
13. ASTM D570-98 (2010). Standard test method for water absorption of plastic

14. Zhang, F, Wang A, Li Z, He S., &Shao, L. (2012). Preparation and characterization of collagen from freshwater fish scales. *Food and Nutrition Sciences* Vol. 2: 818-823.
15. Christensen, P. A., Curtis, T. P., Egerton, T. A., Kosa, S. A. M., & Tinlin, J. R.;1; (2003). Photoelectrocatalytic and photocatalytic disinfection of *E. coli* suspensions by titanium dioxide. *Applied Catalysis B-Environmental*, 41, 371-386.
16. Ashkarran, A. A. (2011). Antibacterial properties of silver-doped TiO<sub>2</sub> nanoparticles under solar simulated light. *Journal of Theoretical and Applied Physics*, 4, 1-8.
17. Fajar, L.B. & Decky J. I. (2018).Water Absorption of Chitosan, Collagen, and Chitosan/Collagen Blend Membranes Exposed to Gamma-Ray Irradiation. *Iranian Journal of Pharmaceutical Sciences*;14 (1): 57-66.
18. Ahmed, M. A., Abdelbar, N. M., & Mohamed, A. A. (2018). Molecular imprinted chitosan-TiO<sub>2</sub> nanocomposite for the selective removal of rose bengal from wastewater. *International journal of biological macromolecules*; 107, 1046-1053.
19. Nasreen, K., Vijayalakshmi, T., Gomathi, S., Anbalagan S. and P. N. Sudha (2013). Synthesis, characterization and study on the water absorption capacity of binary blends of chitosan. *Der Pharmacia Lettre*, 5 (5):145-150.
20. Saja, S., Al-T., Haider, R. S., Abdul Amir, H. K., & Mohd, S. T. (2019). The influence of titanium dioxide nanofiller ratio on morphology and surface properties of TiO<sub>2</sub>/chitosan nanocomposite. <https://doi.org/10.1016/j.rinp.102296>